SCIENCE CHINA
Information Sciences

• **Supplementary File** •

Breaking the responsivity-speed dilemma of a-GaO_x photodetector by alternating gate modulation

Zhongfang Zhang[1], Pengju Tan[1], Xiaohu Hou[1], Xiaolan Ma[1], Mengfan Ding[1], Shunjie Yu[1], Guangwei Xu[1], Xiaolong Zhao[1*] & Shibing Long[1*]

[1]*School of Microelectronics, University of Science and Technology of China, Hefei* 230026, *China*

Appendix A Supplementary Material Figures

The Supplementary Material Figures A1-6 mentioned in the main text are exhibited, related to the detailed device performance measurements.

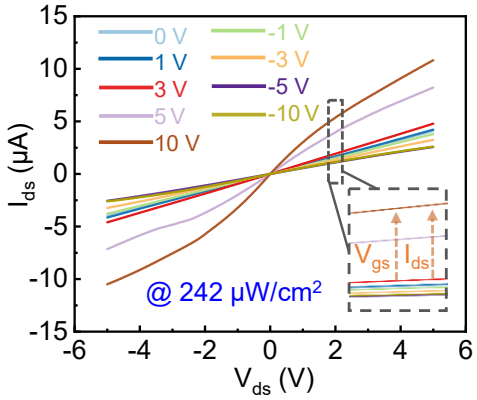

Figure A1 The influence of gate voltage on output photoresponse curves (linear scale). The gate-dependent photocurrent increases with the V_{gs} towards positive.

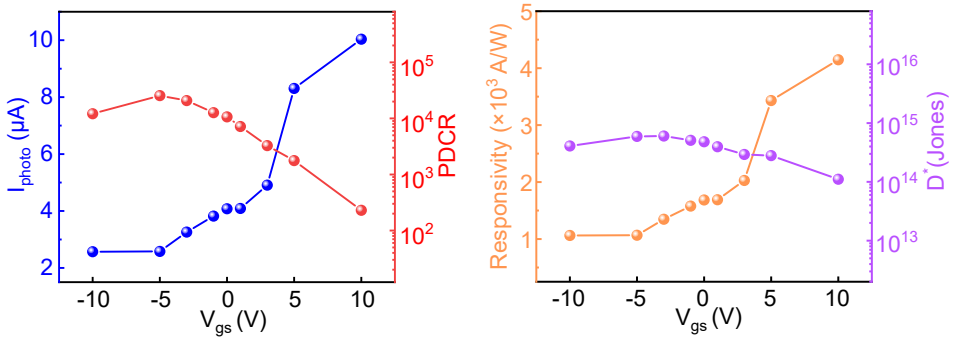

Figure A2 The dependence of photocurrent, $PDCR$, responsivity (R) and detectivity (D^*) on V_{gs}. The R characterizes the photoelectric conversion efficiency of the photodetector, which is usually defined as the photogenerated current per unit power of the incident light absorbed by a certain area, namely R=$(I_{photo}$-$I_{dark})/PS$, where P is the optical power density and S is the total area of active layer of the photodetector. The D^* evaluates the minimum detectable signal of the photodetectors, which can be simply expressed as D^*=$R(S/2qI_{dark})^{1/2}$, where q is the elementary charge.

* Corresponding author (email: xlzhao77@ustc.edu.cn, shibinglong@ustc.edu.cn)

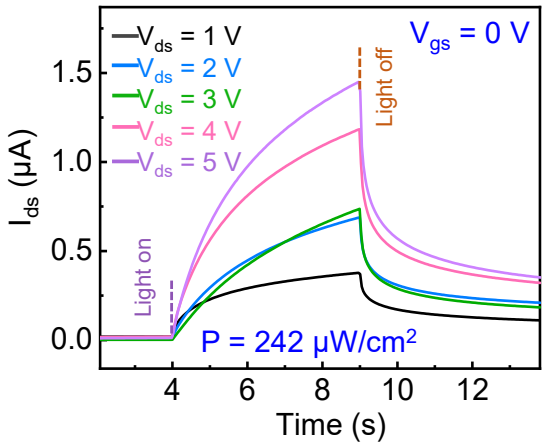

Figure A3 Dependence of Ids-t curves on various V_{ds}. The I_{ds}-t response curves exhibit a faster upward slope and improved I_{photo} with the increment of V_{ds} from 1 V to 5 V.

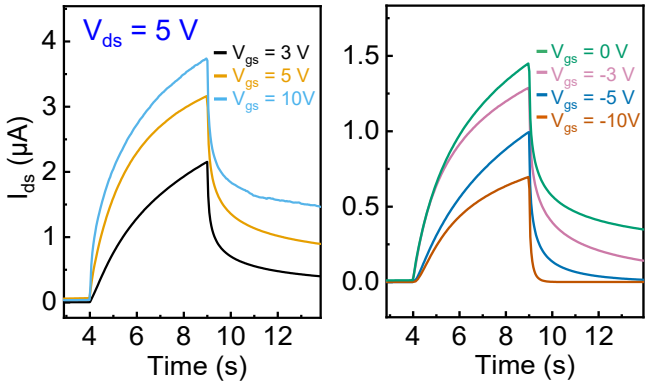

Figure A4 Dependence of I_{ds}-t curves on various V_{gs}. The I_{ds}-t response curves exhibit a faster upward slope and improved I_{photo} with the advance ofV_{gs} from -10 V to 10 V (V_{ds}=5 V).

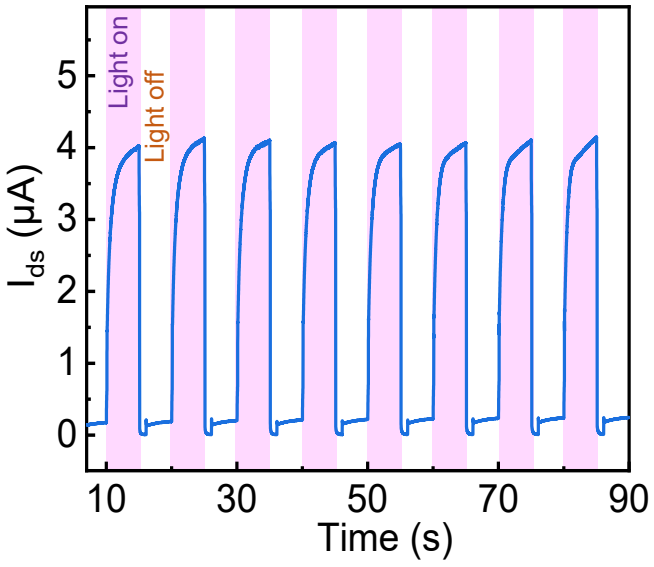

Figure A5 I_{ds}-t curve of the AGM scheme under successive response periods. The recurrent response curves triggered by periodic light pulses with an on/off (5 s/5 s) switching evidence that the AGM scheme possesses great repeatability and stability.

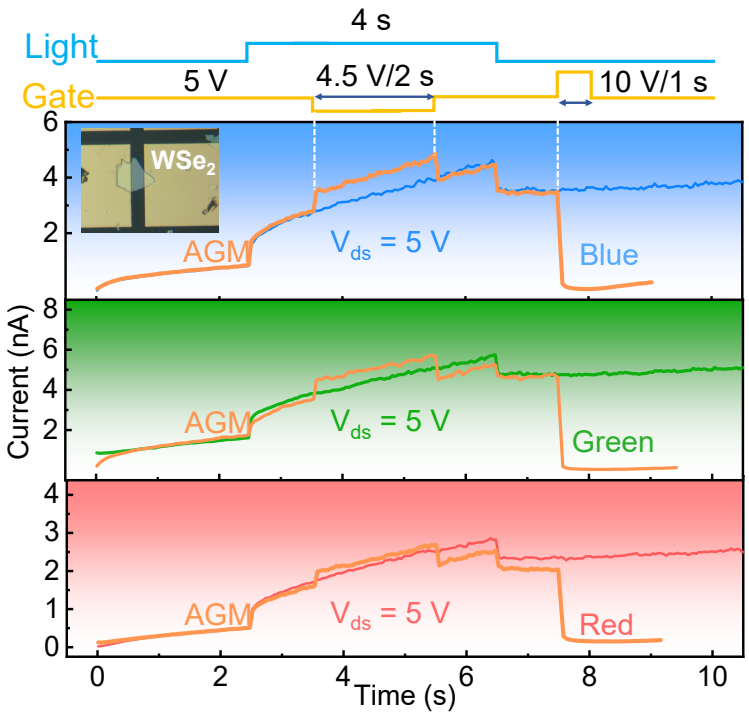

Figure A6 Verification of the universality of the AGM scheme for wide-spectrum p-WSe_2 photodetector. The inset shows an optical microscope photograph of the p-WSe_2 device. AGM schemes are applied on mechanically exfoliated p-WSe_2 photodetector for visible light detection, including blue, green and red. Different from an n-type FET, AGM woking on a p-type FET utilizes a smaller voltage to enhance the responsivity and a larger voltage to erase the photocurrent, thus realizing the dynamic alternation of merits.

Appendix B Methods

Appendix B.1 Fabrication

After the first lithography process, the a-GaO_x thin film was deposited onto the low-resistance p-type Si substrate by RF-magnetron sputtering at room temperature. Separated a-GaO_x films were obtained after the lift-off process. After another lithography process, the source and drain electrodes consisting of Ti/Au (20/50 nm) were deposited onto the a-GaO_x thin film by electron beam evaporation.

Appendix B.2 Device Characterizations

All the I-V and I-t basic curves were characterized by a B1505 semiconductor analyzer at room temperature. The light switching was controlled by a mechanical shutter (THORLABS SBH-025), modulated by a pulse generator unit in B1505.

Appendix B.3 Imaging simulation

The colormap data referred to the measurements in Figure 1(d), and were simulated by an exponential function model as I=A+B exp(-t/τ). For each scheme, the response and decay processes were fitted by different exponential functions based on the I-t curves. When a pixel is under illumination, there will be a response function to calculate the final current; while for a pixel under darkness, there will be a decay function to calculate the final current. The currents of the previous frame were the initial values for the next frame.